Electronic Supplementary Material (ESI) for Energy & Environmental Science.
This journal is © The Royal Society of Chemistry 2016

Supporting Information

Polypyrrole-assistant Oxygen Electrocatalysis on Perovskite Oxides

Dong-Gyu Lee,[a] Su Hwan Kim,[a] Se Hun Joo,[a] Ho-Il Ji,[b,c] Hadi Tavassol,[c] Yuju Jeon,[a] Sihyuk Choi,[c] Myeong-Hee Lee,[a] Chanseok Kim,[a] Sang Kyu Kwak,[a] Guntae Kim,[a] Hyun-Kon Song*,[a]

Experimental Section

Material Preparation. Two different double perovskites (NBSC and NBSC*) were prepared. NBSC was synthesized by sol-gel method. Stoichiometric amounts of $Nd(NO_3)_3 \cdot 6H_2O$, $Ba(NO_3)_2$, $Sr(NO_3)_2$ and $Co(NO_3)_2 \cdot 6H_2O$ were dissolved in distilled water with proper amount of Pluronic F-127. All chemical was used as received from Aldrich. The solution was dried in the oven at 100 ^oC for one day. The precursor gel was heated up to 300 ^oC in air. Fine powders obtained during the combustion were calcined at 600 ^oC for 4 h and then sintered in air at 950 ^oC for 4 h. For measuring intrinsic electrical conductivity, the powder was pressed into pellets at 5 MPa and sintered in air at 1100 ^oC for 12 h instead of the thermal treatment at 950 ^oC for 4 h to achieve a relative density higher than 95 %. Smaller-size NBSC* was prepared by electrospray process. The same precursors used for NBSC were dissolved at 0.01 M each in N,N-dimethylformamide (DMF), followed by introducing 15 wt. % PVP (polyvinylpyrrolidone, Mw = 1,300,000) into the solution. The precursor solution was placed in a 30 ml syringe with a positively charged capillary tip with a diameter of 0.5 mm. 10 kV voltage was applied between the syringe needle tip as an anode and a metal collector wrapped with aluminum foil as a cathode with a gap at 11 cm by a high-voltage power supply (Korea Switching). The composite droplets were electrosprayed from

the needle at 0.3 ml h^{-1} and collected on the aluminum foil. The electrosprayed powders were dried at 80 ^{o}C for 1 h in air and then calcined at 3 ^{o}C min^{-1} ramping to 800 ^{o}C for 4 h in air.

Physicochemical characterization. The crystallographic structures of materials were characterized at a scan rate of 0.6 degree min^{-1} with the 2θ range of 20 ^{o} to 60 ^{o} by X-ray diffraction (XRD; Rigaku diffractometer D/MAZX 2500V/PC with Cu Kα radiation). Scanning electron microscopy (SEM; FEI Nanonova 230) was used to snapshoot their morphologies. Electrical conductivities were measured in air by a four-point probe configuration. Ag wires as probes were connected to samples by Ag paste. The current/voltage was controlled/measured by a potentiostat (BioLogic VMP3) in a temperature range of 25 to 700 ^{o}C.

Electrode preparation. Catalyst inks were prepared by dispersing a catalyst and a conducting agent in 0.45 ml of ethanol, 0.45 ml of isopropyl alcohol and 0.1 ml of 5 wt. % nafion solution (Sigma-Aldrich 274704). The total amount of the catalyst and the conducting agent was fixed at 20 mg. A series of NBSCs were used as the double perovskite catalysts: NBSC and NBSC*. BSCFO was used as the simple perovskite counterpart. Carbon black (C; Akzo Nobel Ketjenblack 600JD) or its composite with polypyrrole (pPy/C; Sigma-Aldrich 530573) was used as the conducting agent at 0, 5 and 20 wt. %. 5 ul of the catalyst ink was dropped on the disk compartment of ring-disk electrodes. Loading density of the composite of catalyst and conducting agent was fixed at 0.8 mg cm^{-2}. For comparison, 20 wt. % platinum nanoparticles supported by carbon black (Pt/C; Premetek P10A200) was used as a control.

Electrochemical characterization. Cyclic and linear sweep voltammograms (CVs and LSVs) were obtained on disk and ring electrodes simultaneously by a bipotentiostat (iviumstat, Ivium Technologies). Ring-disk electrodes (RRDE) of glassy carbon disk and platinum ring was used as

the working electrode (disk area = 0.1256 cm^2) while a platinum wire and a Hg/HgO electrode were used as the counter and reference electrodes respectively. The RRDEs were rotated at various controlled speeds (1600 rpm unless otherwise indicated) by a RRDE controller (ALS RRDE-3A). An aqueous solution of 0.1M KOH was used as the electrolyte. ORR polarization curves were obtained on the disk electrode from a cathodic sweep from +0.1 V to -0.7 V (vs. Hg/HgO) at 10 mV s^{-1} after five cycles of CVs. The electrolyte was saturated by oxygen for ORR while it was purged by nitrogen to measure background currents. +0.4 V was applied to the ring electrode to estimate the amount of peroxide generated from the disk electrode. The anodic sweeps from +0.35V to +0.9V (vs. Hg/HgO) after nine cycles were presented as OER polarization curves. The other conditions were the same as those for the ORR polarization curves. To demonstrate the stability of OER, anodic and cathodic sweeps were repeated at 50 mV s^{-1} for 100 cycles. The values of potential were converted from versus Hg/HgO to versus the reversible hydrogen electrode (RHE) by: Hg/HgO + 0.929 V = RHE. For the correction, the potential difference between Hg/HgO and RHE was measured in a cell where platinum wires were used as the working and counter electrodes in a hydrogen-saturated aqueous electrolyte of 0.1 M KOH with Hg/HgO as the reference electrodes. The open circuit potential was read at -0.929 V vs. Hg/HgO from a LSV at 1 mV s^{-1}.

pPy electrodeposition. 20mM pyrrole was dissolved in 0.1M $LiClO_4$ (aq). Three electrodes were immersed in the electrolyte: NBSC-loaded disk electrode (area = 0.1256 cm^2) of a rotating ring-disk electrode (RRDE) as a working electrode, a platinum wire as a counter and a Ag/AgCl electrode as a reference. The same catalyst ink as described above was used for loading NBSC for the working electrode. Pyrrole was electro-polymerized on the working electrode in the N_2-saturated electrolyte. Potential was swept at 5 mV s^{-1} between +0.2 $V_{Ag/AgCl}$ to +0.8$V_{Ag/AgCl}$ one,

three and five times by a potentiostat (Ivium Iviumstat). The loading amounts of pPy on the NBSC working electrodes were calculated from the charges consumed for electrodeposition under the assumption that positive charges are developed in pPy every three monomeric unit.

pPy-O_2 interaction. pPy films were electrodeposited on gold-coated quartz crystal resonators for quartz crystal microbalance (QCM; SEIKO QCM922) and on carbon screen-printed electrodes (Zensor, SE100; area = 0.196 cm^2) for infrared-spectroscopic (FTIR; Bruker Alpha) measurement. Pyrrole was electrochemically polymerized at 0.1 mA $cm^{-2}$for 150s in 0.1 M pyrrole in 0.1 M NaCl (aq). Then, the pPy films were de-doped at -0.5$V_{Ag/AgCl}$ for 20s. Frequencies of the pPy-deposited resonators were recorded as a measure of mass along time in nitrogen-purged or oxygen-saturated deionized water.

Zn-air batteries. Coin-type zinc-air batteries (2032; diameter = 20 mm) were assembled with 6M KOH (aq) as an electrolyte, zinc plate as an anode, 0.05 g cm^{-2}catalyst-carbon composite loaded on carbon paper as a cathode. NBSC, NBSC+pPy/C or Pt/C was used as the catalyst for cathodes. Discharge curves were obtained at 20mAcm^{-2}.

DFT calculations. Density functional theory (DFT) calculations were performed using Vienna Ab-initio Simulation Package (VASP)[1-2]. The generalized gradient approximation with Perdew-Burke-Ernzerhof functional (GGA-PBE)[3] was employed for the exchange correlation energy. The electron-ion interaction was described by projector augmented-wave (PAW)[4] method. The cutoff energy for the plane wave basis set was set to be 400 eV. Spin polarization and Grimme's D2 dispersion correction[5] were considered in all calculations. The convergence criteria for self-consistent field (SCF) calculations was set to be 10^{-5} eV. The atomic positions and lattice parameters were relaxed until the Hellmann-Feynman forces acting on ions were less than 0.02

eV/Å. 3 × 3 × 3and 3 × 3 × 1 *k*-point meshes with Monkhorst-Pack scheme were used for bulk and surface systems, respectively. Bader charge analysis[6-8]wasimplemented to investigate the atomic charges.

Modeling and calculation details

The unit cell of $Nd_4BaSr_3Co_8O_{24}$ (NBSC) double perovskite was constructed by replacing one Sr atom by one Ba atom in $Nd_4Sr_4Co_8O_{24}$ (**Figure S9**). The lattice parameters of the optimized unit cell were determined as a = 7.53 Å, b = 7.61 Å, c = 7.51 Å, α = 90.73°β = 90.00°, and γ = 90.00°. Using the optimized unit cell, a symmetric slab model of (001) surface consisting of 7 atomic layers was constructed with the vacuum slab of 20 Å (**Figure S9**). Two atomic layers at the bottom were fixed during optimization to consider the bulk-like effect. To elucidate the role of the pPy for the adsorption of O_2 on NBSC surface, we constructed three model systems (i.e., O_2+pPy, NBSC+O_2 and NBSC+O_2+pPy) as shown in **Figure 3c-e**. The interaction between O_2 and pPy was investigated by O_2+pPy system, which was constructed by placing O_2 near N-H bond of pPy. The pPy-assisted O_2 adsorption on the NBSC surface was investigated by comparing NBSC+O_2 and NBSC+O_2+pPy systems, where O_2 was placed above the 5-coordinated Co ion and the pPy was placed above O_2.

The adsorption energy (ΔE_{ad}) of O_2 for three systems was calculated as follows,

$$\Delta E_{\mathrm{ad}} = E_{\mathrm{O_2+pPy}} - E_{\mathrm{pPy}} - E_{\mathrm{O_2}} \quad (1)$$

$$\Delta E_{\mathrm{ad}} = E_{\mathrm{NBSC+O_2}} - E_{\mathrm{NBSC}} - E_{\mathrm{O_2}} \quad (2)$$

$$\Delta E_{\mathrm{ad}} = (E_{\mathrm{NBSC+O_2+pPy}} - E_{\mathrm{NBSC}} - E_{\mathrm{O_2+pPy}}) - (E_{\mathrm{O_2+pPy}} - E_{\mathrm{pPy}} - E_{\mathrm{O_2}}) \quad (3)$$

where E_{O_2+pPy}, E_{NBSC+O_2}, and E_{NBSC+O_2+pPy} represent the total energy of each system and E_{NBSC}, E_{O_2}, and E_{pPy} represent the energy of isolated NBSC surface, O_2, and pPy respectively. Note that the first and second term of equation (3) represent the interaction energy between NBSC and O_2+pPy and that between O_2 and pPy, respectively. Thus, we can calculate adsorption energy of O_2 on NBSC surface by subtracting those two terms.

References for DFT calculation

1. G. Kresse and J. Furthmüller, *Physical Review B*, 1996, **54**, 11169-11186.
2. G. Kresse and J. Furthmüller, *Comp Mater Sci*, 1996, **6**, 15-50.
3. J. P. Perdew, K. Burke and M. Ernzerhof, *Physical Review Letters*, 1996, **77**, 3865-3868.
4. G. Kresse and D. Joubert, *Physical Review B*, 1999, **59**, 1758-1775.
5. S. Grimme, *J Comput Chem*, 2006, **27**, 1787-1799.
6. W. Tang, E. Sanville and G. Henkelman, *J Phys-Condens Mat*, 2009, **21**.
7. E. Sanville, S. D. Kenny, R. Smith and G. Henkelman, *J Comput Chem*, 2007, **28**, 899-908.
8. G. Henkelman, A. Arnaldsson and H. Jonsson, *Comp Mater Sci*, 2006, **36**, 354-360.

Table S1 | The bifunctionality of perovskite oxide catalysts.

Catalysts	$E_{ORR}(V_{RHE})$ at -3 mA/cm^2	$E_{OER}(V_{RHE})$ at +10 mA/cm^2	ΔE (V)	Ref
$NdBa_{0.2}Sr_{0.8}Co_2O_{3-\delta}$ with pPy[1a,2a]	0.79	1.65	0.86	This work
$NdBa_{0.2}Sr_{0.8}Co_2O_{3-\delta}$[1a,2a]	0.61	0.71	1.10	This work
$Ba_{0.5}Sr_{0.5}Co_{0.8}Fe_{0.2}O_{3-\delta}$[1a,2a]	0.55	1.79	1.24	This work
$Nd_{0.5}Sr_{0.5}CoO_{3-\delta}$/GnP nanorods [1a,2a]	0.70	1.72	1.02	[1]
$LaNiO_3$/NC[1a,2a]	0.65	1.61	0.96	[2]
$La_{0.5}Sr_{0.5}CoO_{2.91}$ Nanowires[1b,2a]	0.77	1.83	1.06	[3]
$La_{0.9}Sr_{0.1}CoO_3$ Yolk–shell[1a,2a]	0.69	1.79	1.10	[4]
$La_{0.5}Sr_{0.5}Co_{0.8}Fe_{0.2}O_3$/NCNT[1a,2b]	0.53	1.70	1.17	[5]
$La_{0.8}Sr_{0.2}Mn_{0.6}Ni_{0.4}O_3$[1a,2a]	0.47	1.78	1.31	[6]
$La_{0.7}(Ba_{0.5}Sr_{0.5})_{0.3}Co_{0.8}Fe_{0.2}O_{3-\delta}$[1a,2a]	0.62	1.62	1.00	[7]
$LaNiO_{3-\delta}$[1b,2a]	0.59	1.65	1.04	[8]
Pt/$CaMnO_3$[1b,2a]	0.85	1.83	0.98	[9]
$La_{0.95}FeO_{3-\delta}$[1b,2a]	0.47	1.66	1.28	[10]

[1]Scan rate: 1a = 10 mV sec^{-1}; 1b = 5 mV sec^{-1} [2]Rotation speed: 2a = 1600 rpm; 2b = 900 rpm.

References for Table S1

1. C. Kim, O. Gwon, I. Y. Jeon, Y. Kim, J. Shin, Y. W. Ju, J. B. Baek and G. Kim, *J. Mater. Chem. A*, 2016, **4**, 2122.
2. W. G. Hardin, D. A. Slanac, X. Wang, S. Dai, K. P. Johnston and K. J. Stevenson, *J. Phys. Chem. Lett.*, 2013, **4**, 1254.
3. Y. L. Zhao, L. Xu, L. Q. Mai, C. H. Han, Q. Y. An, X. Xu, X. Liu and Q. J. Zhang, *Proc. Natl. Acad. Sci. U. S. A.*, 2012, **109**, 19569.
4. S. Y. Bie, Y. Q. Zhu, J. M. Su, C. Jin, S. H. Liu, R. Z. Yang and J. Wu, *J. Mater. Chem. A*, 2015, **3**, 22448.
5. H. W. Park, D. U. Lee, M. G. Park, R. Ahmed, M. H. Seo, L. F. Nazar and Z. W. Chen, *Chemsuschem*, 2015, **8**, 1058.
6. J. C. Scott, P. Pfluger, M. T. Krounbi and G. B. Street, *Phys. Rev. B*, 1983, **28**, 2140.
7. J. I. Jung, M. Risch, S. Park, M. G. Kim, G. Nam, H. Y. Jeong, Y. Shao-Horn and J. Cho, *Energy Environ. Sci.*, 2016, **9**, 176.
8. W. Zhou and J. Sunarso, *J. Phys. Chem. Lett.*, 2013, **4**, 2982.
9. X. P. Han, F. Y. Cheng, T. R. Zhang, J. G. Yang, Y. X. Hu and J. Chen, *Adv. Mater.*, 2014, **26**, 2047.
10. Y.-W. Ju, S. Yoo, C. Kim, S. Kim, I.-Y. Jeon, J. Shin, J.-B. Baek and G. Kim, *Advanced Science*, 2016, **3**, 1500205.

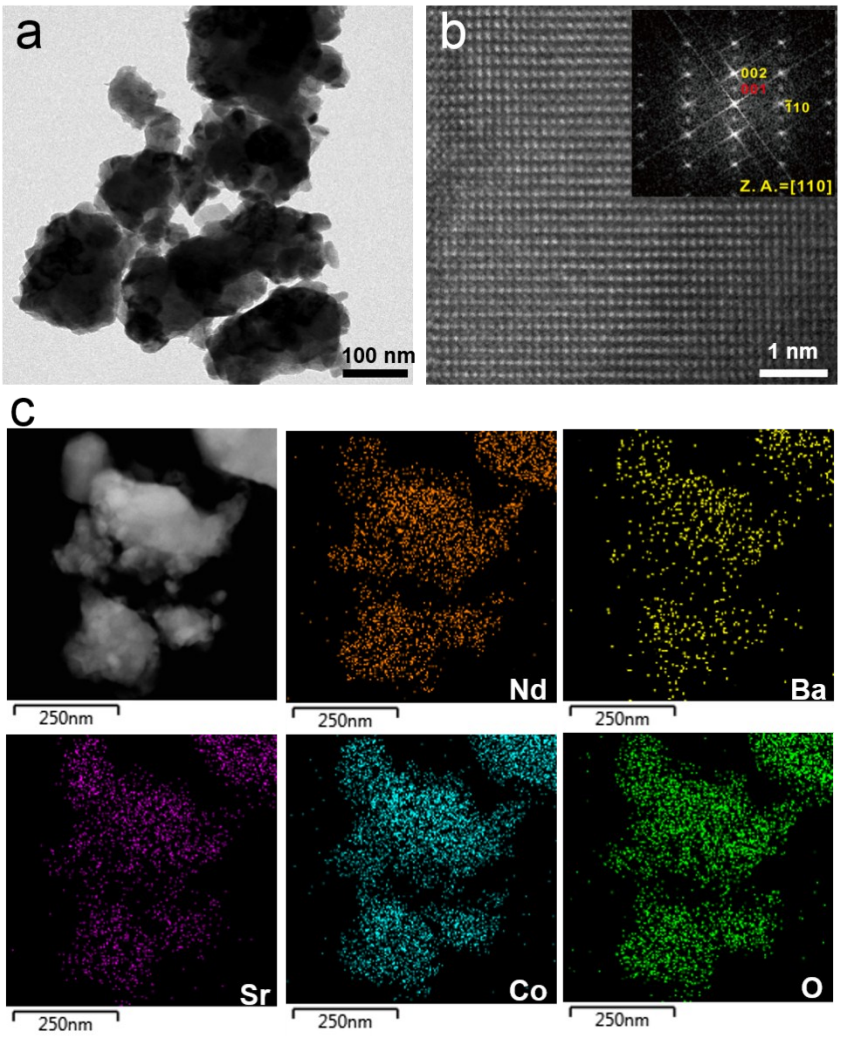

Figure S1 | Electron-microscopic characterization of NBSC. (**a**)A TEM image at low magnification. (**b**) A TEM image at high magnification with its fast Fourier transformed pattern. Spots of weak intensity in the pattern were observed when electron beam was introduced in a [110] direction. They are indexed with (001) of a tetragonal super lattice, indicating the double perovskite structure. (**c**) Element mapping by energy dispersive spectroscopy (EDS). Each component was uniformly distributed throughout particles.

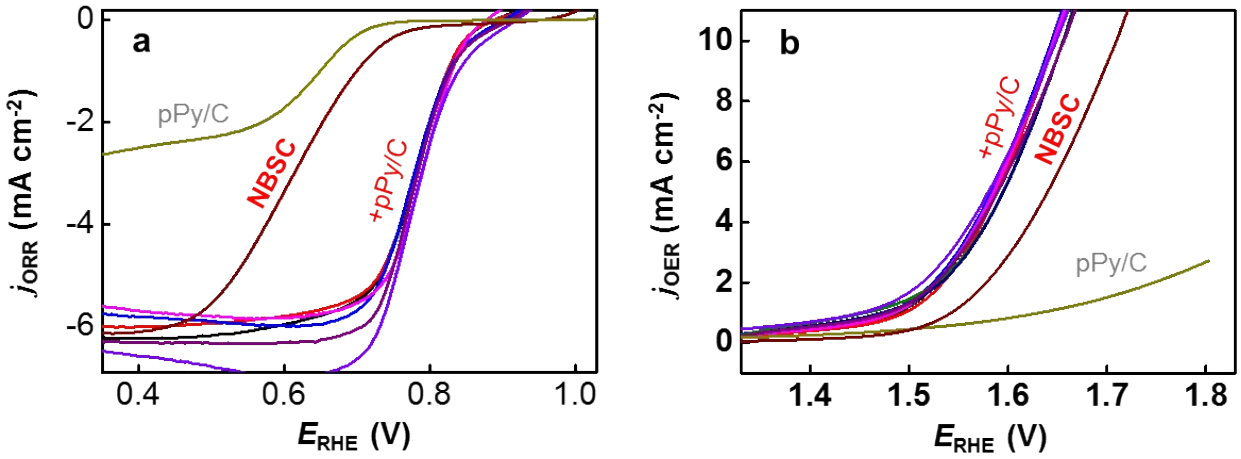

Figure S2 | Reproducibility of the NBSC+pPy/C performances. (a)ORR polarization in 0.1 M KOH (aq) at cathodic scan. (b) OER polarization in 0.1 M KOH (aq) at anodic scan. Scan rate = 10 mV sec^{-1}. Rotation speed = 1600 rpm.

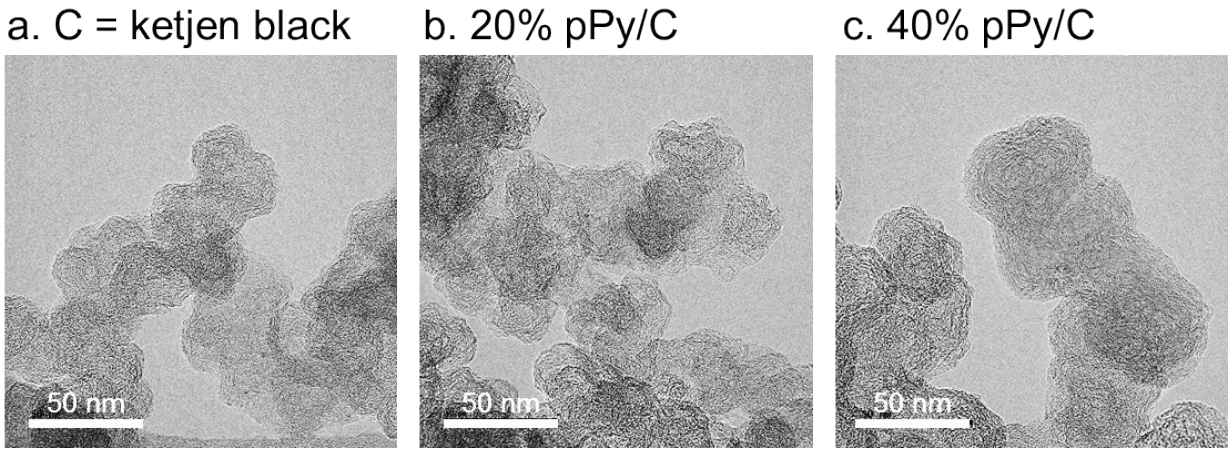

Figure S3 | TEM images of carbon black and pPy/C. (a)C = Ketjen black. (b) 20 % pPy/C. (c) 40 % pPy/C. The scale bars are for 50 nm.

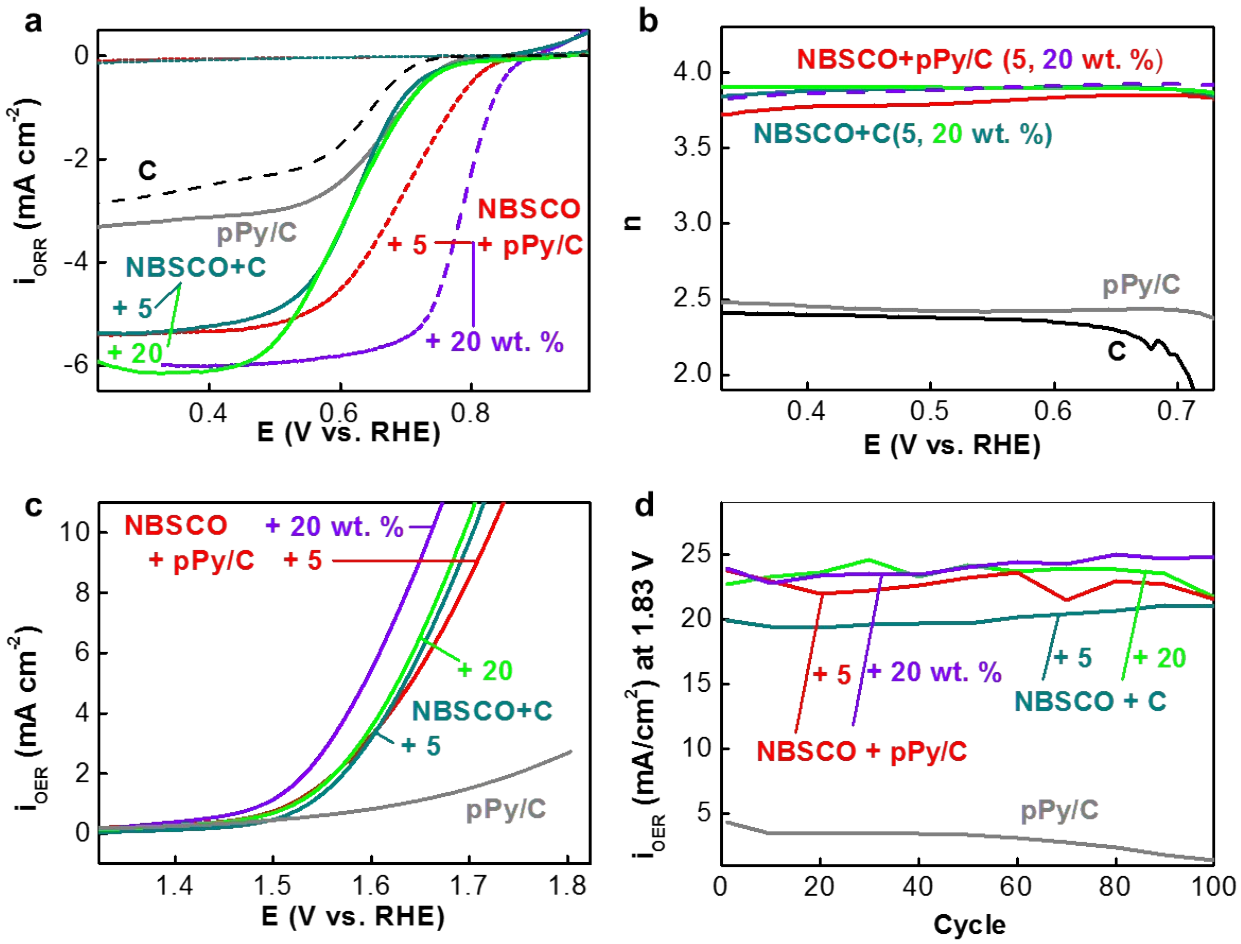

Figure S4| ORR and OER of NBSC in the presence of different conducting agents: carbon (Ketjen black; C) and polypyrrole/carbon black composite (pPy/C). (a)Voltammogram of disk currents of ORR in 0.1 M KOH (aq) at cathodic scan (scan rate = 10 mV sec^{-1}; rotation speed = 1600 rpm). (b) Number of electron transfer (n). (c) Voltammogram of disk current of OER at anodic scan (scan rate = 10 mV sec^{-1}; rotation speed = 1600 rpm). (d) Stability of OER. The OER current (i_{OER}) at 1.83 V vs. RHE was traced along repeated cycles consisting of anodic and cathodic scans between 0.93 V and 1.83 V vs. RHE.

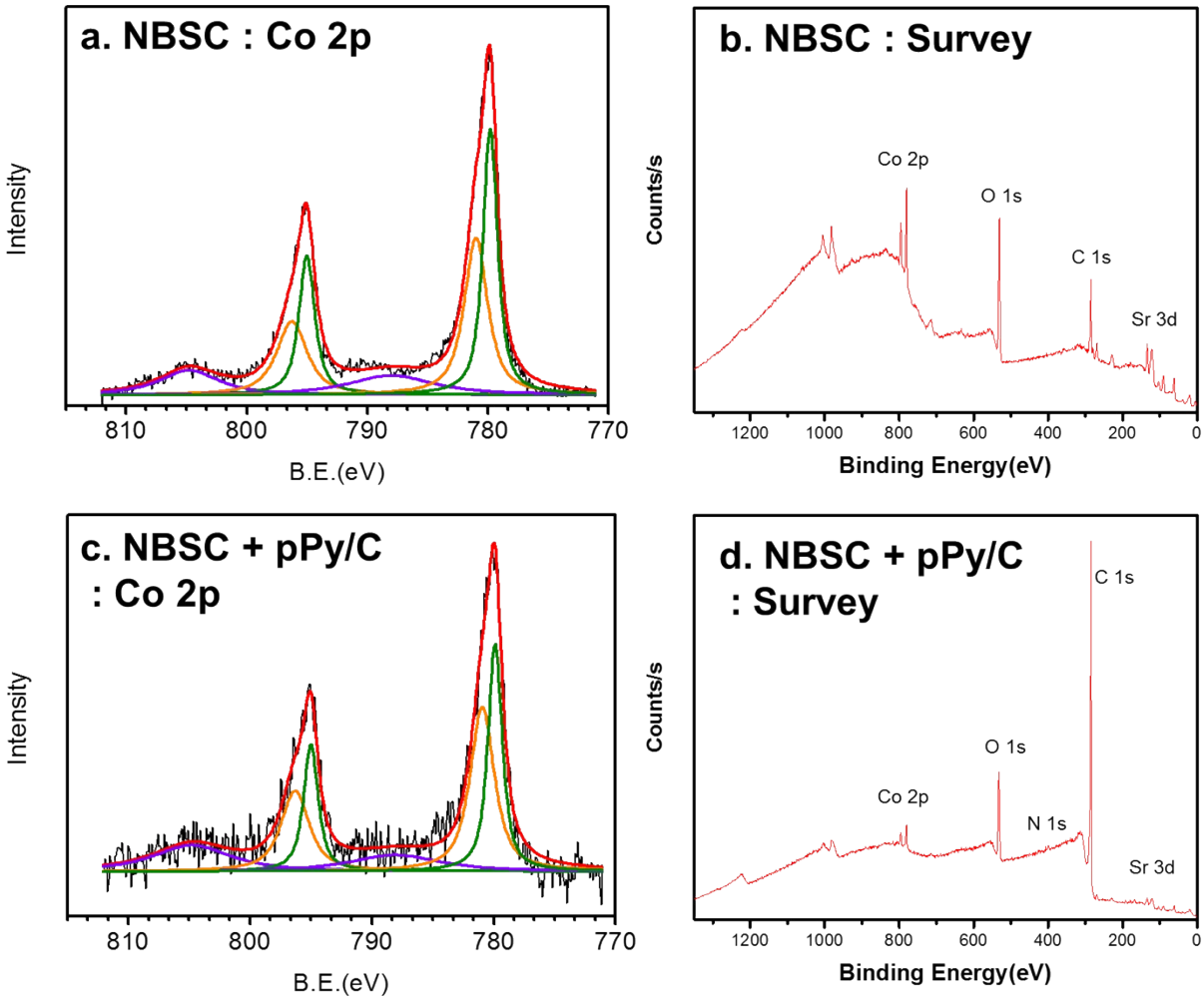

Figure S5 | X-ray photoelectron spectra of Co2pwith the survey spectra. (a, b) NBSC. (c, d) NBSC + pPy/C. There were no difference observed between the two samples.

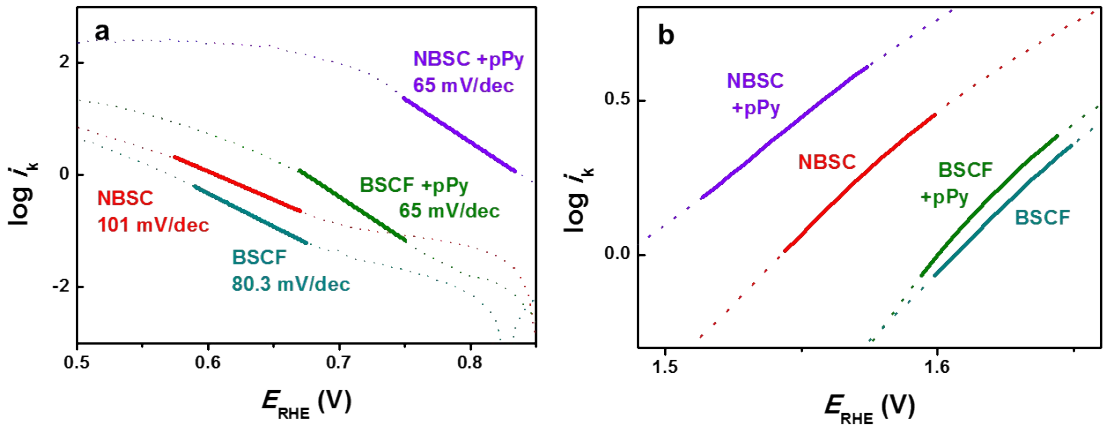

Figure S6 | Tafel plots. (a)ORR. (b)OER.

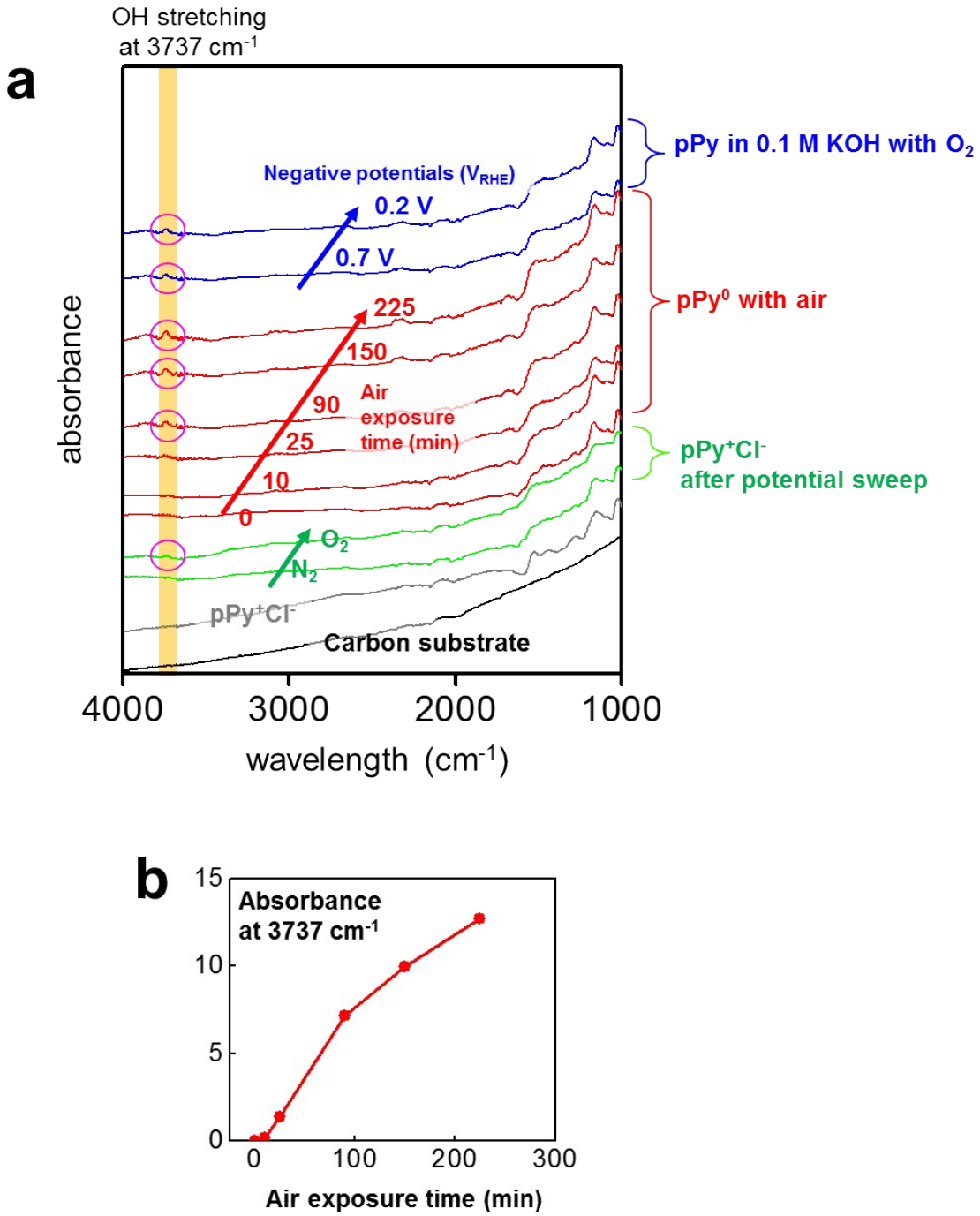

Figure S7 | Spectroscopic characterization of pPy in the presence of O_2. (**a**) Infrared spectra. The peak at 3737cm^{-1} for OH stretching was developed along time when the pPy films were exposed to oxygen or air. (**b**) Temporal change in the absorbance at 3737cm^{-1}.

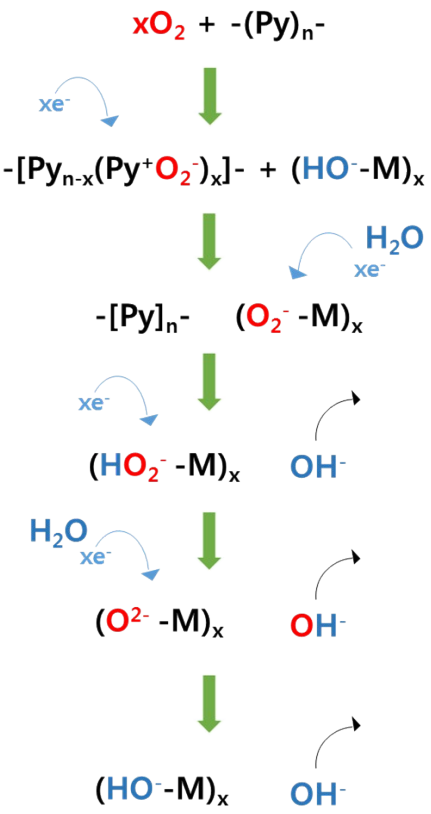

Figure S8 | Proposed mechanism to explain the role of pPy on improved kinetics of ORR.

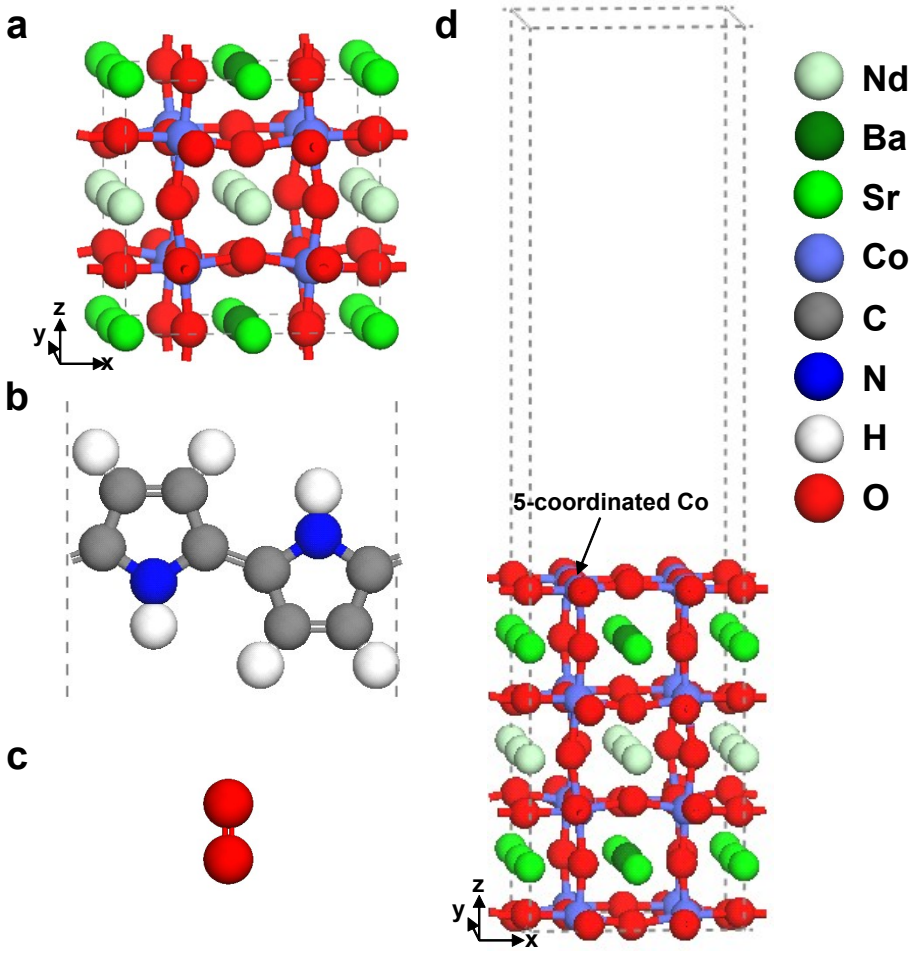

Figure S9 | Optimized structures for DFT calculation. (a) NBSC. (b) pPy. (c) O_2. (d) (001) surface of NBSC. The labels of atomic colors are presented in the figure. The gray dashed line indicates both lattice and periodic boundary.

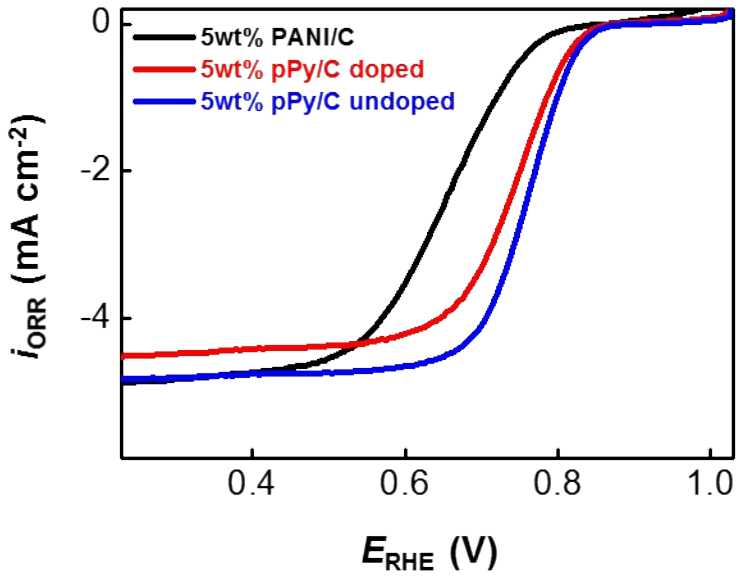

Figure S10 | ORR polarization of NBSC in the presence of nitrogen-containing conducting polymers. Electrocatalytic layers were prepared by introducing 5 wt. % conducting polymer/carbon composites into NBSC. Doped pPy, undoped pPy or polyaniline was used as the conducting polymer. Scan rate = 10 mV sec^{-1}. Rotation speed = 1600 rpm.

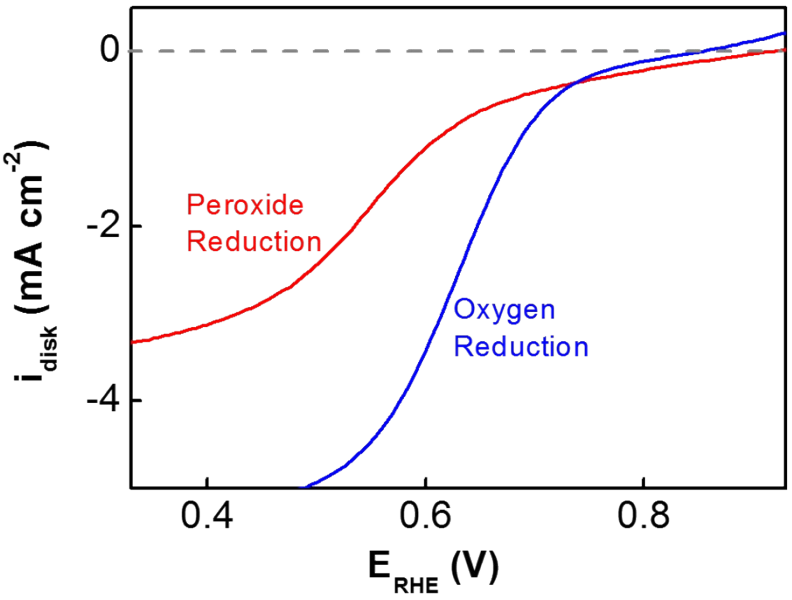

Figure S11 | Polarization of peroxide reduction on NBSC in the presence of 2mMperoxide in 0.1M KOH (aq)(red solid line). Presented for comparison was the ORR polarization on NBSC in oxygen-saturated 0.1M KOH (aq) (blue solid line).Scan rate = 10 mV sec^{-1}. Rotation speed = 1600 rpm.

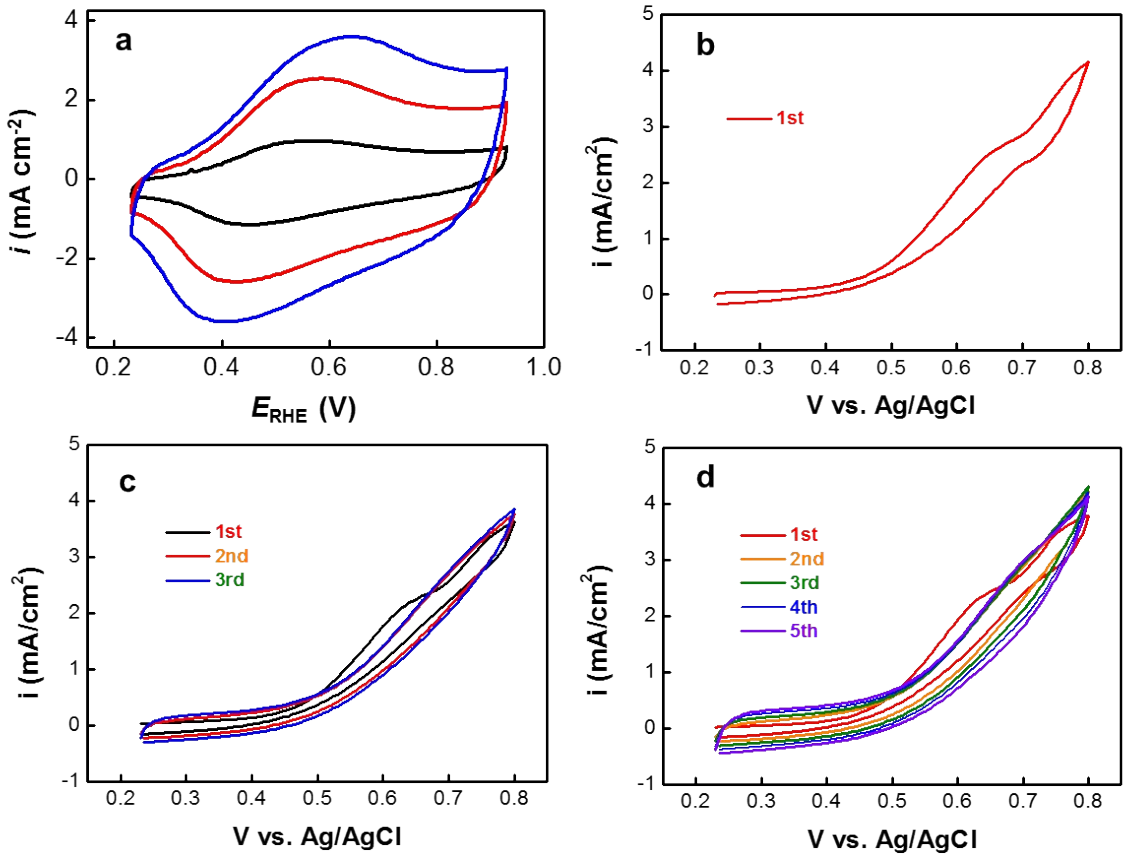

Figure S12 | Electrodeposition of pPy on NBSC+C. (a) Cyclic voltammogram (CV) of the ORR on disk electrode in N_2-saturated 0.1 M KOH (aq) at 10 mV sec^{-1}. Black, red and blue line are pPy03, pPy06 and pPy09.

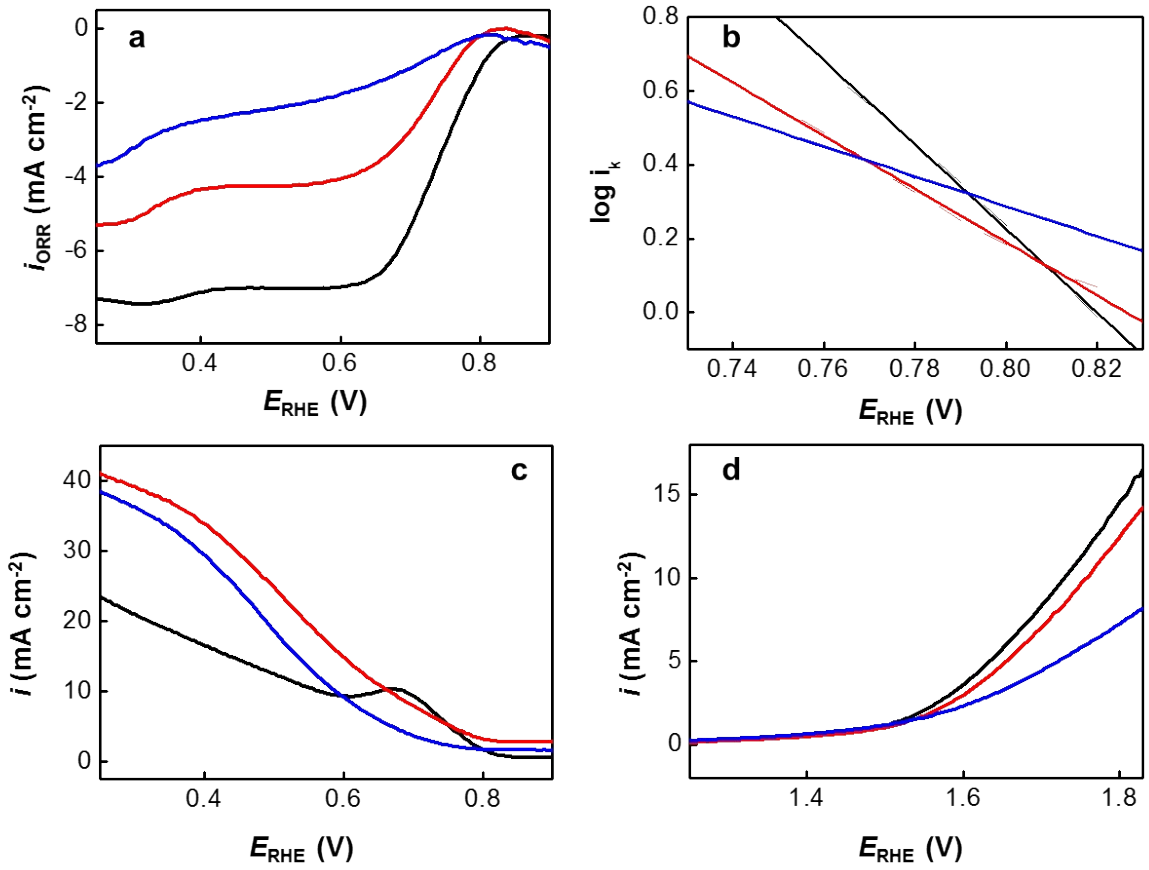

Figure S13 | ORR and OER of pPy/NBSC. Black, red and blue lines are 0.3, 0.6 and 0.9 wt. % of pPy on NBSC catalyst layer, respectively. (a) ORR polarization in 0.1 M KOH (aq) at cathodic scan (scan rate = 10 mV sec^{-1}; rotation speed = 1600 rpm). (b) Tafel plots. (c) Voltammogram of ring current of re-oxidization at 0.4V. (d) OER polarization at anodic scan (scan rate = 10 mV sec^{-1}; rotation speed = 1600 rpm).

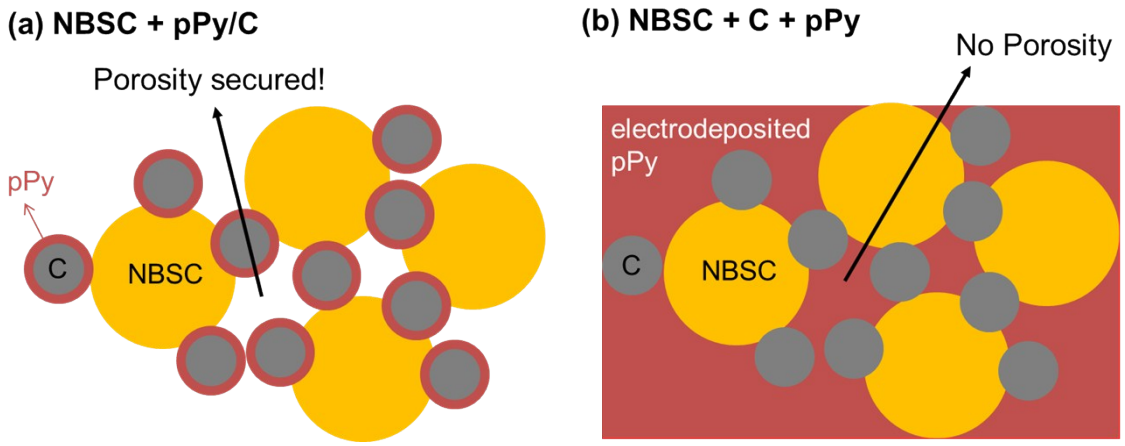

Figure S14 | NBSC + pPy/C versus NBSC + C + pPy. It should be notified that the pPy-deposited system (**Figure 4**) includes carbon (C) because pPy was electrodeposited on a mixture of NBSC and C (NBSC+pPy+C). The ORR kinetics was faster in NBSC+pPy/C (**Figure 1a**) than in NBSC+pPy+C (**Figure 4a**) when comparing the slopes of current increase before the limiting situation between the two systems. Electric conductivity would not be significantly different between NBSC+pPy/C and NBSC+C+pPy. However, the major difference comes from mass transfer. The use of pPy/C guarantee the porosity between the particles of NBSC and pPy/C. On the contrary, pPy films could block the ionic pathways existing between NBSC and C in the NBSC+C+pPy system.